Journal of Electroceramics, 13, 239–243, 2004

Frequency and Voltage Dependent Dielectric Properties of Ni-doped $Ba_{0.6}Sr_{0.4}TiO_3$ Thin Films

MI-HWA LIM,[1] HYUN-SUK KIM,[1] NAN-YOUNG KIM,[1] HO-GI KIM,[1] IL-DOO KIM,[2,*]
SEUNG EON MOON,[3] MIN-HWAN KWAK,[3] HAN-CHEOL RYU[3] & SU-JAE LEE[3]

[1] *Department of Materials and Science and Engineering, Korea Advanced Institute of Science and Technology, 373-1 Guseong-dong, Daejeon, 305-701, South Korea*

[2] *Crystal Physics and Electroceramics Laboratory, Massachusetts Institute of Technology, 77 Massachusetts Avenue, Cambridge, MA 02139, USA*

[3] *Basic Research Lab., Electronics and Telecommunications Research Institute, 161 Kajeong, Yuseong, Daejeon, 305-350, South Korea*

Submitted September 4, 2003; Revised January 29, 2004; Accepted January 30, 2004

Abstract. Highly (100) preferred undoped and 1–5% Ni-doped $Ba_{1-x}Sr_xTiO_3$ (BST) thin films were deposited onto MgO (100) single crystal substrate at 750°C using pulsed laser deposition. BST thin film-based interdigital capacitors (IDC) were prepared by standard photolithography process. The microwave properties of BST films were measured at 10 GHz. Ni-doped BST films showed better dielectric properties by exhibiting improved dielectric Q while retaining an appropriate capacitance tuning compared to undoped BST films. 1% Ni-doped BST film showed the maximum figure of merit of 2896.1. It is suggested that 1 mol% Ni doped BST film is an effective candidate for high performance tunable device applications.

Keywords: BST, Ni doping, microwave, interdigital capacitor

1. Introduction

$Ba_{1-x}Sr_xTiO_3$ (BST) is being investigated with considerable interest as a dielectric material for dynamic random access memories (DRAM) [1] and more recently for tunable microwave device applications such as electrically tunable mixers, delay lines, filters, capacitors, oscillators, resonators and phase shifters [2–4]. Frequency and phase agility in these circuits are achieved through the ferroelectric thin film's relative dielectric constant (ε_r) which shows nonlinear response to an applied dc electric field. Here, tunability is defined as $\varepsilon_r(\max)/\varepsilon_r(\min)$, where the relative dielectric constant at zero bias is represented by $\varepsilon_r(\max)$, and $\varepsilon_r(\min)$ is the relative dielectric constant at a higher or defined field. The tunable dielectric constant results in a change in the phase velocity in the device allowing it to be tuned in real time for a particular application. In tunable microwave devices, it is desirable to have a high dielectric tunability and a low dielectric loss. However, as it is not easy to obtain high tunability and low loss tangent simultaneously, compromises are needed between them in order to optimize the reasonable tunability and loss tangent of the BST tunable devices. Undoped BST thin films have high tunabilities upward of 50% at bias voltage of less than 10 V in the low frequency range. But, the relatively high dielectric loss of the BST films, especially at microwave frequencies, has precluded their use. It was well documented that small amounts of doping materials such as Mg, Mn, Fe ions can remarkably influence the electrical properties of capacitors. However, there has been few reports of characterization of Ni-doped BST films at high frequency range of GHz. In this study, Ni-doped BST films were deposited onto MgO (100) substrates at 750°C by pulsed laser deposition (PLD). The behavior of microwave properties in the BST films with Ni doping concentration at high frequencies (1–10 GHz) was investigated using an interdigital capacitor. This work demonstrates a potential use for 1 mol% Ni-doped BST thin films in tunable microwave devices.

*To whom all correspondence should be addressed. E-mail: idkim@mit.edu

2. Experimental

Undoped and Ni-doped (1, 2, 5 mol%) $Ba_{0.6}Sr_{0.4}TiO_3$ (BST) thin films of 500 nm thick were grown on MgO (100) single crystal substrates by PLD (pulsed laser deposition). The substrate temperature and oxygen ambient pressure was 750°C and 50 mTorr, respectively. The laser ablation was carried out at a laser fluence of 1.5 J/cm^{2}and a repetition rate of 5 Hz using KrF excimer source ($\lambda = 248$ nm). The electrode, a 2 μm thick gold layer, was deposited on the BST film to complete the circuit fabrication. To enhance the adhesion between the BST thin film and the gold electrode [5], a thin Cr adhesion layer was deposited prior to Au deposition. The final geometries of the interdigital capacitor (IDC), similar to those of Ref. [6], were achieved by standard photolithography process. As shown in Fig. 1, The IDC structure consists of 10 pairs of fingers that are 20 μm wide, 3–10 μm apart, and finger overlap length of 300 μm. The crystallinity and the structure of the BST films were determined by X-ray diffractometry (XRD, Rigaku D/max-rc) excited with Cu K_α radiation. The microstructure and roughness of the BST films were observed by scanning electron microscopy (SEM, Philips XL30SFEG) and atomic force microscopy (AFM), respectively. Microwave property measurements were made with an HP 8510C vector network analyzer using one port measurement in the frequency range of 1 to 10 GHz.

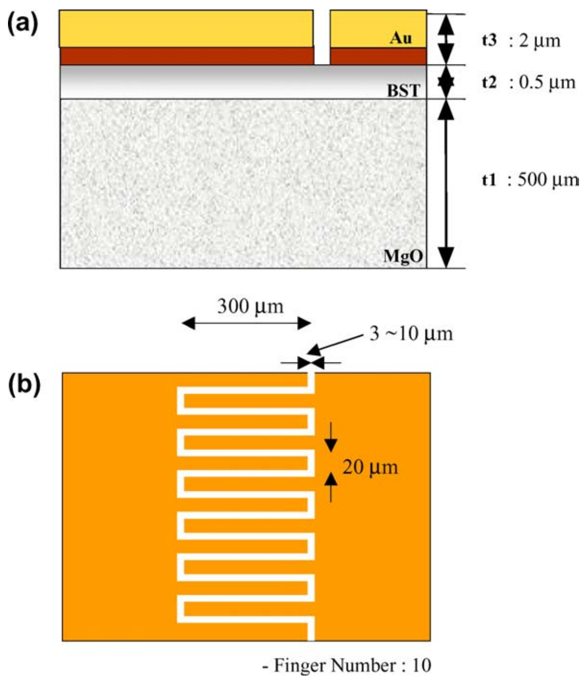

Fig. 1. Schematic diagram of (a) cross-section of a interdigital capacitor Au/Cr/BST/MgO and (b) top interdigital electrode structure.

3. Results and Discussion

Figure 2 illustrates the XRD patterns for BST thin films with different Ni concentrations, showing only the (100) and (200) peak of the BST film. This figure reveals that the (100) plane is dominant in the BST films. Discrete diffraction spots with fourfold symmetry were observed when a BST (110) plane was used as the diffraction plane. This indicates that all (undoped and doped) BST films grew epitaxially on MgO (100) substrates. Typical full width at half-maximum (FWHM) for the (200) reflection of BST films on MgO (100) substrates varies from 0.97 to 1.19°. The undoped BST film had the minimum FWHM as 0.97° and the Ni-doped BST films had relatively larger values. This result shows that the crystallinity of the BST films decreases with adding Ni doping. This may be understood from the fact that the incorporation of divalent Ni ions

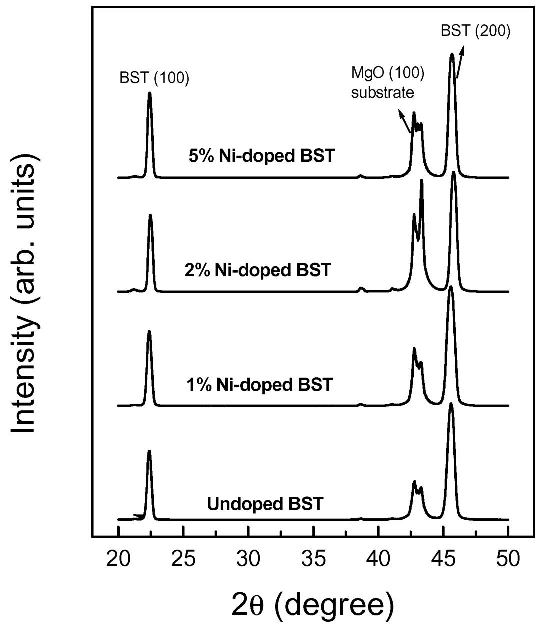

Fig. 2. X-ray diffraction patterns for the undoped and Ni-doped BST films grown on MgO(100) substrate.

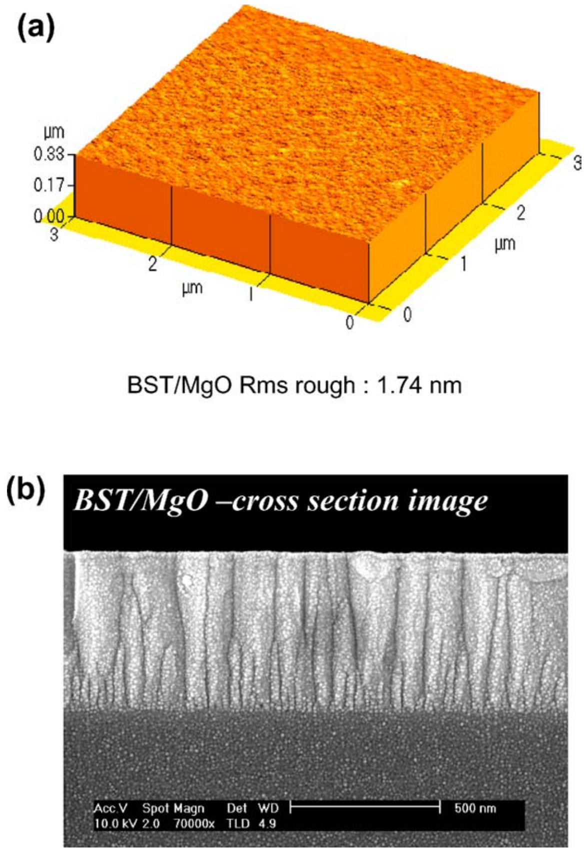

Fig. 3. (a) AFM image of surface morphology of BST film grown on MgO substrate and (b) SEM cross-section image of BST/MgO structure.

needs higher solution energies to form compensating point defect [7].

Figure 3(a) shows a typical result obtained with 3-D atomic force microscopy of surface morphology for an area of 3×3 μm. The Rms value of the thickness was 1.74 nm for BST films grown on MgO substrates. From cross-sectional images in Fig. 3(b), a typical columnar structure with very fine and uniform grain size was observed.

Electrical and dielectric properties of the BST films were obtained through the investigation of interdigital capacitors with the configuration of Ar/Cr/BST/MgO. We measured the microwave frequency tuning properties of the BST films at 10 GHz using an HP 8510C network analyzer. The tuning properties were obtained with the applied electric field up to 133 kV/cm.

Figure 4 shows the measured result of the capacitance as a function of the gap width. The tuning range

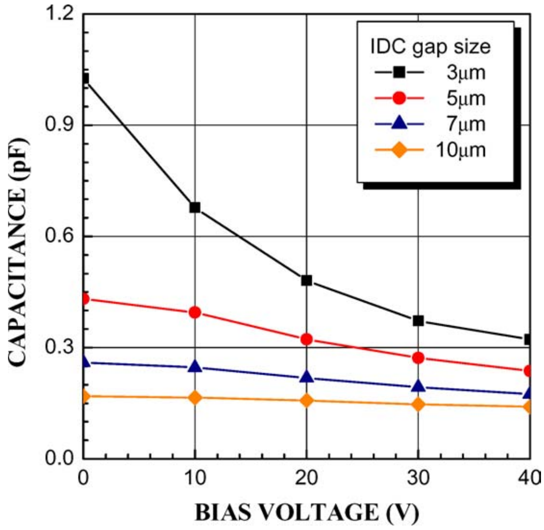

Fig. 4. Capacitance-voltage characteristics as a function of dc bias voltage of IDC with different gap width.

of the IDC increased as the gap width decreased since the dc electric field strength increases as the gap width decreases. At the applied electric field of 133 kV/cm (40 V), the tunability values of BST films grown on MgO were 68.7 and 16.9% with 3 μm and 10 μm gap width IDCs, respectively. In order to compare the film's quality with varied dielectric properties for application in microwave tunable devices, the use of a figure of merit (FOM) (% tuning $\times$ Q_{0V}, where Q_{0V} is Q (quality factor) at 0 kV/cm) is important.

Figure 5 shows the FOM values and the Q measured at 10 GHz as a function of the gap width. While the capacitance tuning at 10 GHz tends to decrease as the gap size increases, the quality factor Q increased with the increase of gap width. As shown in Fig. 5, the IDC with 3 μm gap size showed the highest FOM value of 1566. On the basis of the results, in order to obtain high performance IDC properties, we fabricated IDC structures with 3 μm gap size to investigate the Ni doping effect on BST films.

Figure 6 shows the capacitance dependence of the undoped and Ni-doped BST thin films as a function of external bias voltage from 0 to 40 V (electric field from 0 to 133 kV/cm) at a frequency of 10 GHz. As shown in Fig. 6, Ni doping had a great influence on the properties of the BST films. Undoped and 1% Ni-doped BST films have higher capacitance and thus dielectric constant than those of 2 and 5% Ni-doped BST films. At an applied voltage of 40 V, the tunability values

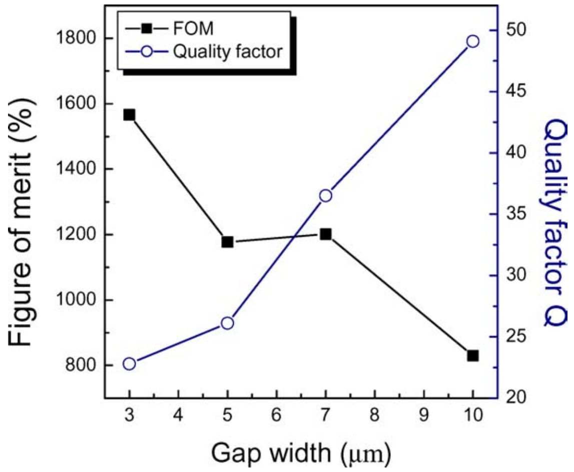

Fig. 5. The variation of FOM and Q measured at 10 GHz as a function of gap width at applied dc bias voltages up to 40 V.

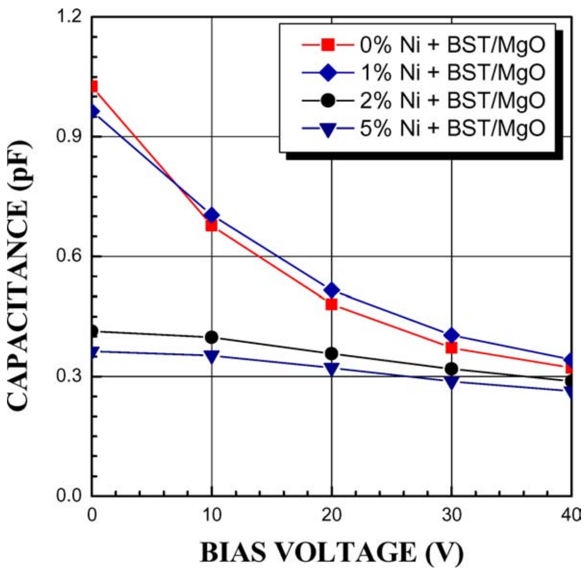

Fig. 6. Capacitance-voltage characteristics as a function of dc bias voltage of IDC with various Ni doping concentration.

of undoped, 1, 2, 5 mol% Ni-doped BST films were 68.7, 64.5, 30.3, 27.5, respectively. Figure 7 shows the variation of the figure of merit (FOM) and quality factor (Q) measured at 10 GHz as a function of the Ni doping concentration. The Q factor is observed to increase (that is, dielectric loss decreases) from 22.8 to 57.6 with increasing Ni doping concentration. The 1% Ni-doped BST film showed the highest K value of 2896.1. These results agree with previous reports

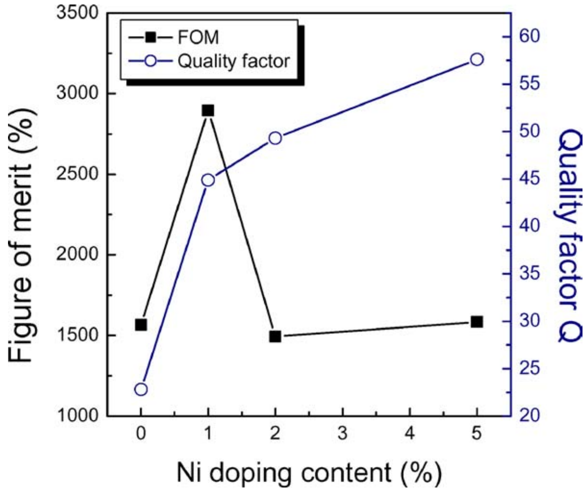

Fig. 7. The variation of FOM and Q measured at 10 GHz as a function of Ni doping concentration at applied dc bias voltages up to 40 V.

on acceptor doped BST thin films. Generally, Mn^{3+}, Ni^{2+}, Ni^{3+}, and Mg^{2+}, which can occupy the B site of the $A^{2+}B^{4+}O_3^{2-}$ perovskite structure, have been known to lower the dielectric loss [8–10]. On the basis of the similar ionic radii between $Ti^{4+}(r_{\text{eff}} = 0.61$ A) and $Ni^{2+}(r_{\text{eff}} = 0.69$ A) in sixfold coordination, we can assume that Ni occupies Ti in the BST lattice with doubly ionized oxygen vacancy is simultaneously formed.

$$NiO \xrightarrow{TiO_2} Ni_{Ti} + O_O + V_O^{\cdot\cdot} \quad (1)$$

where $V_O^{\cdot\cdot}$ is an extrinsic oxygen vacancy created to compensate charge by the Ni addition. Ni behaves as an acceptor-type dopant, which can prevent reduction of Ti^{4+} to Ti^{3+} by neutralizing the donor action of the oxygen vacancies. Because electrons can hop between neighboring titanium ions thus provide a mechanism for dielectric loss. Ni acceptor dopants help to lower the loss tangent. At the high temperatures and low oxygen partial pressures used to deposit BST films, reduction occurs, resulting in n-type conductivity in the prepared films according to the following equation [11].

$$O_O \rightarrow V_O^{\cdot\cdot} + 2e' + \frac{1}{2}O_2(g) \quad (2)$$

Where O_O, V_O, and e' represent the oxygen ion on its normal site, oxygen vacancy, and electron, respectively. The increase of the oxygen vacancy concentration created by NiO addition eventually causes a decrease in the concentration of electron. This decrease in electron density can lead to lower leakage currents in BST films.

In accordance with these arguments, the leakage current density of Ni doped BST films grown on LSCO/Pt electrodes decreased with increasing Ni doping concentration [12].

4. Conclusions

We demonstrated that NiO can be an effective dopant for decreasing dielectric loss and increasing the figure of merit of BST films making them more suitable for application in microwave tunable devices. We have shown that the tunability values of undoped, 1, 2, 5 mol% Ni-doped BST films were 68.7, 64.5, 30.3, 27.5 at an applied electric field of 133 kV/cm, respectively. 1% Ni-doped BST film showed the highest figure of merit value of 2896.1 through the reduction of the dielectric loss. This study suggests that 1 mol% Ni doped BST thin films appear to be excellent potential candidates for tunable microwave application.

Acknowledgment

This work was supported by the Post-doctoral Fellowship Program of Korea Science & Engineering Foundation (KOSEF) and BK 21 Project.

References

1. A.I. Kingon, S.K. Streiffer, C. Basceri, and S.R. Summerfelt, *Mater. Res. Bull.*, **21**, 18 (1995).
2. F.A. Miranda, F.W. Van Keuls, R.R. Romanofsky, and G. Subramanyam, *Integrated Ferroelectric*, **22**, 269 (1998).
3. W.J. Kim, W. Chang, S.B. Qadri, J.M. Pond, S.W. Kirchoefer, D.B. Chrisey, and J.S. Horwits, *Appl. Phys. Lett.*, **76**, 1185 (2000).
4. I.D. Kim, J.H. Park, M.H. Lim, M.S. Kim, H.G. Kim, S.G. Yoon, K.B. Kim, T.S. Yun, and J.C. Lee, *Jpn. J. Appl. Phys.*, **41**, 7218 (2002).
5. G.M. Smith, D.V. Faobes, R.M. Lammert, and J.J. Colemann, *Appl. Phys. Lett.*, **67**, 3847 (1995).
6. E.K. Kim, S.E. Moon, S.J. Lee, S.K. Han, K.Y. Kang, and W.J. Kim, *Integrated Ferroelectrics*, **272**, 237 (2002).
7. C.J. Peng and S.B. Krupanidhi, *J. Mater. Res.*, **10**, 708 (1995).
8. Y. Xu, *Ferroelectric Materials and their applications* (North Holland, New York, 1991).
9. U.N. Weston, *J. Am. Ceram. Soc.*, **52**, 253 (1969).
10. V.K. Varadan, D.K. Ghodgaonkar, and V.V. Varadan, *Microwave J.*, **30**, 116 (1992).
11. M. Copel, P.R. Duncombe, D.A. Neumayer, T.M. Shaw, and R.M. Tromp, *Appl. Phys. Lett.*, **70**, 3227 (1997).
12. H.S. Kim, M.H. Lim, H.G. Kim, and I.D. Kim, Electrochem. Solid-State Lett., accepted (2003).